

Intensity Fluctuations in Hurricane Gustav

August 30-September 1, 2008

Joseph P. Zagrodnik

University of Wisconsin-Madison
Department of Atmospheric and Oceanic Sciences

5 May 2009

ABSTRACT

Intensity fluctuations in Hurricane Gustav were analyzed from when Gustav was a Category 1 hurricane on August 30, 2008 near Grand Cayman Island until its final landfall in Louisiana on September 1. For the analysis, National Hurricane Center intensity estimates were compared to Gustav's internal and external dynamical interactions, which included ocean temperatures, passage over land, upper level wind shear, dry air entrainment, and eyewall replacement cycles. These processes were all investigated in comparison to the conceptual model of a hurricane as a Carnot heat engine. It was first determined that Gustav's rapid intensification over the Caribbean Sea was due to warm oceanic heat content and enhanced upper level divergence from a trough over the Gulf of Mexico. Secondly, Gustav's land interaction with Cuba was found to be minor due to the island geography's inability to disrupt the storm's inflow. Gustav then passed over the warm Gulf of Mexico loop current but significantly weakened due to wind shear and especially mid level dry air entrainment. Finally, Gustav underwent an eyewall replacement cycle prior to landfall, which contributed to the storm weakening to Category 2 strength upon landfall.

I. Introduction

Forecasting hurricane intensity remains a difficult challenge that has lagged behind hurricane track forecasting. Despite more sophisticated numerical models and higher resolution satellite imagery, the best intensity forecasts are still statistically based methods such as the Dvorak Technique (Wang and Wu, 2004). This remains the case because hurricanes undergo a number of both internal and external dynamical interactions which results in frequent and sometimes rapid changes in intensity. The Maximum Potential Intensity (MPI) of a hurricane can be calculated based primarily on sea surface temperature (SST) but these environmental and dynamical factors keep the actual intensity almost always below the MPI (Camp and Montgomery, 2000). Environmental factors can include upwelling of cold sea temperatures in slow moving storms, entrainment of dry continental airmasses, and vertical wind shear. Dynamical factors can include eyewall replacement cycles and interactions with both internal and environmental Rossby waves (Wang and Wu, 2004).

A number of these intensity modifiers affected Hurricane Gustav on its track from the Caribbean Sea to its final landfall in Louisiana. From a synoptic perspective, the hurricane experienced favorable upper level winds during its intensification periods and moderate southwesterly wind shear during periods when it struggled to gain strength. Dry air also intruded into Gustav's circulation as it entered the Gulf of Mexico, as a trough over the Western Gulf provided low θ_e air from the United States that wrapped into the circulation. On the mesoscale, Gustav's intensification period corresponded with the formation of a closed, circular eyewall with axisymmetric outer bands. The storm also was in the middle of an eyewall replacement

cycle upon landfall, as concentric eyewalls were observed.

Presiding over these intensity modifiers, sea temperatures provided the fuel for Gustav's destructive power but also regulated its intensity at times. This process can be envisioned in terms of a Carnot Cycle, which is the basic conceptual model for a hurricane. The dependency on warm ocean waters can also be examined when considering Gustav's brief pass over western Cuba. This case study will examine each of these intensity factors by comparing previous research to model data and observations from the hurricane in order to explain how each of them either encouraged intensification or prevented Gustav from reaching its MPI.

II. Data

The primary method for analyzing hurricanes is through satellite images. For this study, the GOES 12, 4 km resolution IR imagery was used for monitoring the evolution of the storm. The 10.7 micron IR channel is sensitive to cold, high cloud tops and was therefore used for analyzing the general storm structure and evolution and the extent of the convective bands. The 6.5 micron IR channel is sensitive to water vapor and was used for analyzing Gustav's interaction with a mid to upper tropospheric trough. The 0.67 micron 1 km resolution visible channel was also employed for viewing higher resolution images during daytime hours.

Radar imagery from the New Orleans WSR-88D Doppler was briefly viewed in this study, but the hurricane only approached the US radar network at the end of its lifespan. However, a substitute was available in the form of microwave imagery. The MIMIC (Morphed Integrated Microwave Imagery at CIMSS) analysis

combines five microwave channels to display the inner structure of hurricanes. The images are generally used as a proxy for the distribution of precipitation and therefore can be treated similarly to a radar image.

Synoptic analysis was prepared using the AVN211 model runs from 00 UTC on August 30, 2008 through September 1, 2008 as well as the NAM 104 grid model initialization analysis to view the Caribbean Sea at 12 UTC on August 30. The General Meteorology Package (GEMPAK) and the Gempak Reanalysis and Rendering Program (GARP) were specifically utilized for generating synoptic plots of wind speeds and θ_e . Since the model runs are not a completely accurate representation of reality, especially when analyzing a mesoscale system, it was attempted to compare model data to actual observations and National Hurricane Center (NHC, 2008) forecast discussions as much as possible to determine if any discrepancies existed.

III. Gustav Overview

Figure 1 summarizes Gustav's path, intensity, and the major features that influenced its intensity. Gustav originated from a tropical wave that emerged off the West Coast of Africa on August 14, 2008. The wave first began to organize on August 18, but the storm did not begin significant intensification until nearly a week later on August 24. On August 25, the storm was officially upgraded to a tropical depression. From this time, it took just one additional day for Gustav to become a hurricane and make landfall in Haiti. Gustav maintained tropical storm strength for the next day and very slowly moved southwestward toward Jamaica. The storm gradually picked up speed as it moved directly over Jamaica as a tropical storm on August 29 and then strengthened into a Category 1 hurricane on August 30 as it moved over the Cayman

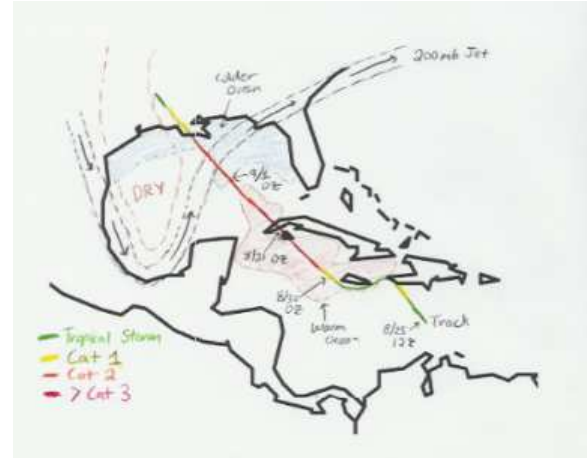


Figure 1: Analysis of Gustav's track and the environmental factors that influenced its intensity.

Islands. Gustav then underwent a period of fast intensification, reaching Category 4 status by late August 30. That night, Gustav struck western Cuba with 150 mph maximum sustained winds. The storm emerged into the Gulf on August 31 as a Category 3 storm, but never regained its previous intensity, as it made its final landfall in western Louisiana as a Category 2 storm on September 1 (NHC, 2008).

While there are a number of interesting aspects to this storm such as the initial development and land interactions, this case study focuses specifically on the August 30-September 1 time period, as Gustav underwent the most drastic intensity changes during this time period. Figure 1 provides a conceptual, Miller Diagram-type schematic of Gustav's track through the Caribbean and Gulf. This diagram summarizes the environmental factors that influenced Gustav's intensity. It is important to note that "warm" and "cold" ocean temperatures refer to the tropical cyclone heat potential, which is different than the actual sea surface temperature. Each of these features will be explained further throughout the analysis.

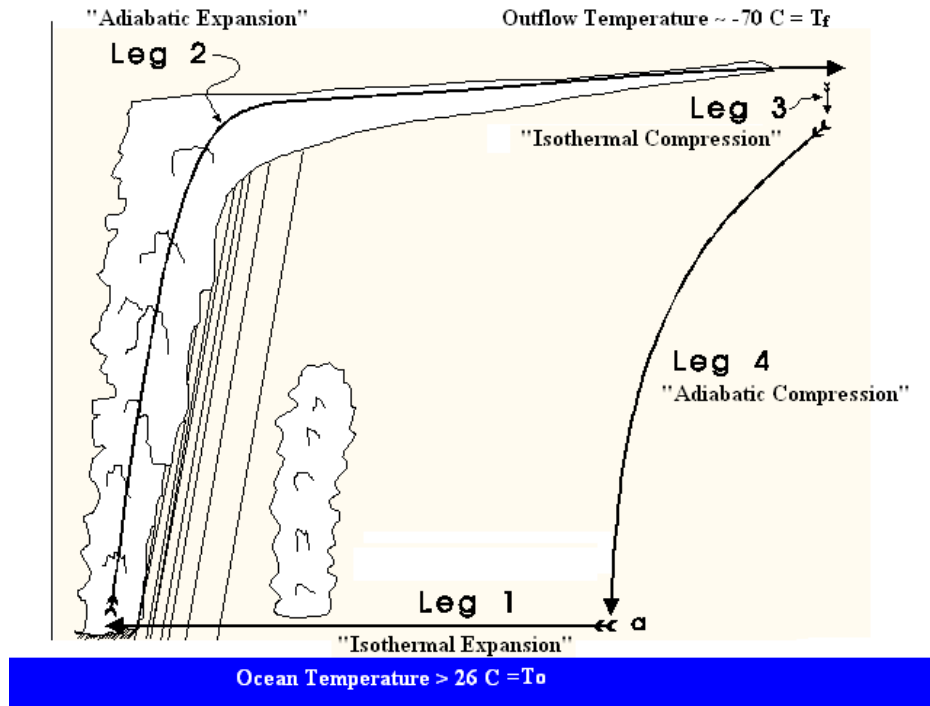


Figure 2: Basic conceptual model of a Carnot heat engine as applied to a hurricane. Modified from Emanuel, 2005.

IV. Ocean Temperatures

a) Carnot Cycle

All intense weather systems derive their energy from inherent temperature instabilities in the earth's climate system. Synoptic systems derive their energy from baroclinic instability, meaning the potential energy present due to the unequal heating between the poles and the equator (Holton, 1979). Thunderstorms extract their energy from Convective Available Potential Energy (CAPE) which arises when a warm, moist positively buoyant layer is situated below a colder, stable layer. In both cases, the potential energy is converted into kinetic energy through latent heat of condensation. Hurricanes also extract energy from the ocean through the same fundamental process. In the tropical oceans, a similar instability develops between the warm ocean waters and the undersaturated tropical atmosphere. A hurricane is very effective at exploiting this instability, as it gathers latent

heat energy by evaporating tremendous amounts of ocean water and then converts the latent heat from the water vapor into mechanical energy within its convection (Emanuel, 1991). The cooler ocean waters left in the wake of a hurricane represent a more stable state than the initial warm waters, which explains why a hurricane needs warm waters to extract energy and persist.

This process of heat transfer in a hurricane can be conceptualized as a closed, four step Carnot Cycle, as seen in Figure 2. Leg 1 of the cycle occurs as boundary layer air spirals inward toward the center of the storm. This leg is referred to as the "isothermal expansion" phase of the cycle, as the air maintains a constant temperature but still gains heat in the form of increased humidity from oceanic moisture transfer. In addition, the pressure in the center of a hurricane is much lower than the surroundings, so the air also expands as it moves inward. Since adiabatic cooling is

prevented by constant heat transfer with the ocean's nearly constant temperature, the result is an incredible energy buildup that can be parameterized through a much increased surface θ_e . The total energy of the incoming air is dramatically increased during this stage, as the enthalpy (heat content) of the ocean is transferred to the atmosphere (Emanuel, 1991).

The second leg of the system occurs as the surface air ascends through convection from the eyewall and flows outward to a very large radius in the lower stratosphere. This stage is referred to as "adiabatic expansion" since the air is no longer in contact with the ocean and does not gain any additional heat. Although the total entropy remains constant, heat energy is converted into mechanical energy through the transfer of latent heat into sensible heat. This occurs when the high θ_e air from the surface condenses into liquid water in the cumulonimbus clouds while the expansion with rising does work on the surroundings. By the end of leg 2, the air has cooled from approximately the same temperature as the sea surface down to around -70°C and has risen to around 12-18 km in height (Emanuel, 2005). At this elevation, the air is neutrally buoyant with respect to the environment.

In the third leg, the air descends slowly downward in the lower stratosphere while losing electromagnetic radiation to space. It is assumed that the loss of heat through radiation balances the gaining of heat through compression, meaning that this stage can be referred to as "isothermal compression" to stay consistent with the Carnot Cycle. The fourth leg is similar to the third leg, as the air continues to lose radiation to space as it descends through the troposphere. It turns out that this radiation loss is nearly equivalent to the amount of heat that would have been lost if all the rainwater in the storm would have remained

in the system and evaporated in leg 4 instead of falling out in leg 2 (Emanuel, 2005). This assumption works as long as the ocean acts as an unlimited heat reserve and continues to provide water vapor to the system, which it generally does this as long as the hurricane keeps moving. Therefore, the final phase is one of "adiabatic compression" and the cycle is closed.

b) Efficiency and Maximum Potential Intensity

If one accepts the assumption that a hurricane is essentially a Carnot Cycle, then the thermodynamic efficiency (ϵ) can be calculated as $(T_f - T_o) / (T_f)$ where T_f is the temperature of the cold pool and T_o is the temperature of the warm pool. In the hurricane's conceptual model (Figure 2), T_f is the average outflow temperature of the top of the convection while T_o is the ocean SST. In a typical hurricane, the thermodynamic efficiency is around 1/3 (Emanuel, 1991). One can derive a maximum potential wind speed equation by combining the thermodynamic efficiency equation with equations for the rate of dissipation of kinetic energy and the rate of heat input per unit surface area. The results of this equation, derived by Kerry Emanuel, can be compared to T_f and T_o as seen in Figure 3.

Using the GOES 12 $10.7\ \mu\text{m}$ satellite temperature over the coldest cloud tops compared to the sea surface temperature, one can compare Gustav's intensity to Figure 3. When Gustav was a Category 4 hurricane approaching Cuba on August 30 at 2130 UTC, the cloud tops around the eye were around $202\ \text{K}$ (-71°C). The SST over this region was around 30°C at the time (AOML, 2008). This data set is plotted on Figure 3 as point "A" which reveals a maximum potential wind speed around 85 m/s, or about 190 mph. As Gustav approached Louisiana on September 1 at

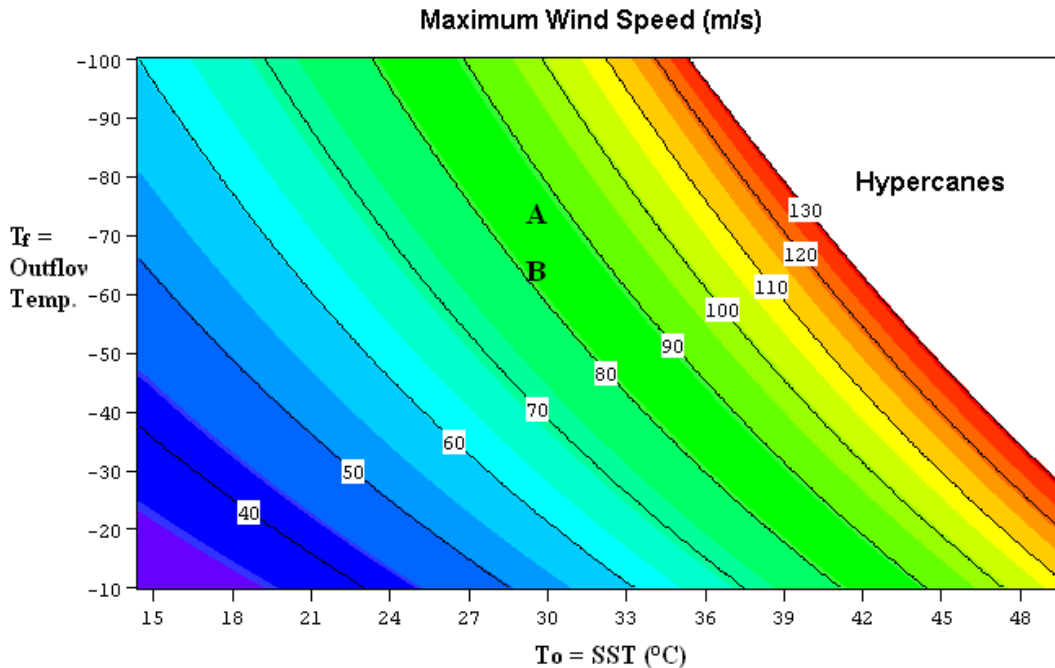


Figure 3: Maximum potential hurricane wind speed in m/s as a function of Carnot cycle inflow temperature (SST) and outflow temperature (cloud top temperature). Point “A” is for Gustav over the Caribbean Sea and “B” is for Gustav approaching Louisiana. Modified from Emanuel, 1999.

0930 UTC, the cloud tops around the eye warmed to an average of about 208 °K (-65 °C). The SST was 29 °C over this region so point “B” on Figure 3 reveals the maximum wind speed is reduced to about 80 knots (179 mph). This analysis reveals that the maximum potential intensity is generally much higher than the actual intensity, as Gustav only had one minute maximum sustained winds of 67 m/s (150 mph) at the time of point “A” and 51 m/s (115 mph) at the time of point “B” (NHC, 2008). The MPI works well as a measure of potential strength, but actual intensity is much more complicated.

c) Sea Surface Temperature (SST)

As mentioned, sea surface temperatures are the primary regulator of a hurricane’s intensity, but they only establish a maximum bound on intensity. Even though the Gulf of Mexico and Caribbean Sea had SST values in the 29-30 °C range, the actual heat content of the ocean mixed

layer varied quite dramatically over Gustav’s path. This is primarily due to the loop current, which transfers warm subtropical waters into the Gulf of Mexico as part of the North Atlantic subtropical gyre. The loop current contains only slightly warmer surface water than the ambient Gulf SST, but the warm water extends much deeper in the loop current (Shay et al., 1999). The deeper source of warm water is important since a hurricane effectively mixes the ocean layer. Some of this mixing is due to turbulence from surface wave breaking, but most of it is due to the vertical shear of the ocean current velocity caused by surface frictional transfer from the hurricane’s winds. The most drastic decreases in SST occur behind and to the right of a hurricane, but the SST can be reduced by a few degrees Celsius underneath the eye, especially if the mixed layer is not enhanced by the subtropical gyre (Emanuel, 2005).

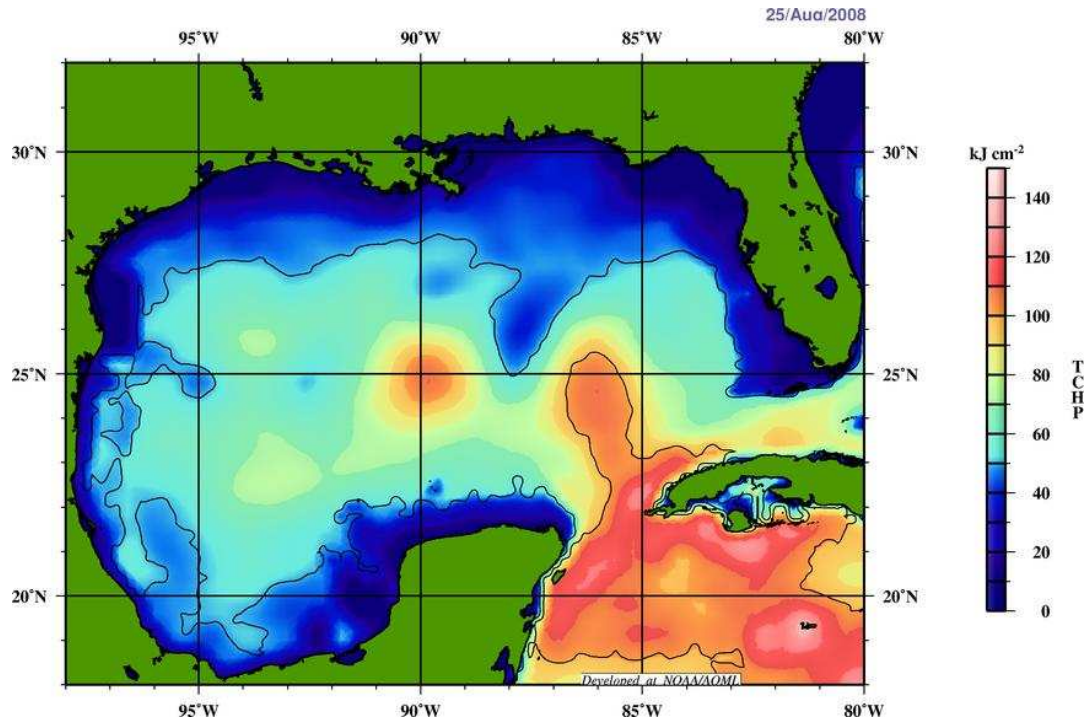


Figure 4: Tropical Cyclone Heat Potential (TCHP) measured in KJ/cm^2 over the Gulf of Mexico and Northern Caribbean Sea. Analysis done on August 25, 2008, which was right before Gustav moved through. Reproduced from AOML, 1998.

In order to take into account the entire mixed layer sea temperature, an algorithm known as Tropical Cyclone Heat Potential (TCHP) has been created to develop a more accurate measure of potential intensity than simple SST values. TCHP is simply a measure of the integrated vertical temperature from the sea surface to the depth of the 26°C isotherm (AOML). Figure 4 shows the TCHP from August 25, right before Gustav moved through in energy per unit area (KJ/cm^2). The loop current is well defined as it moves through the Straights of Yucatán while a secondary warm feature is centered farther to the west. This is likely a warm eddy which broke off of the loop and gradually drifted westward (Emanuel, 2005). Comparing Figure 4 to Figure 1, Gustav crossed waters with a very high heat potential between Grand Cayman Island and Cuba, which directly coincides with its period of strongest intensification. Gustav recorded a 38 mb mean sea level

pressure (MSLP) fall from 980 mb on 00 UTC August 30 as it crossed Grand Cayman to 942 mb 24 hours later on 00 UTC August 31 as it was about to make landfall in Cuba. This strengthening only fell 4 mb short of intensification of 42 mb in 24 hours needed to classify this as an official rapid intensification event (NHC Glossary).

In the Gulf of Mexico, the correlation between TCHP and Gustav's intensity is much more complicated. The Gulf only has a TCHP comparable to the Caribbean ($\sim 100 \text{ KJ}/\text{cm}^2$) in the loop current, with much lower values elsewhere. Gustav's track took it directly over the loop current, then through a cold eddy, and finally through moderately warm water before landfall. The storm maintained Category 4 strength after moving over Cuba, but made landfall in Louisiana as only a strong Category 2 storm. This final intensity conflicted with the National Hurricane Center forecast, which initially predicted

only minor weakening and landfall as a major hurricane. The reason the forecast overestimated the final strength was that Gustav actually weakened over the loop current, as the maximum sustained winds fell from 140 mph to 115 mph. This indicates that although the loop current can result in rapid intensification, as seen with Hurricane Katrina in 2005, an increase in maximum potential intensity does not necessarily correspond with an increase in actual intensity.

d) Land Interaction

One possible way to explain Gustav's inability to re-strengthen over the loop current is that the storm's circulation was significantly disrupted by its passage over Cuba. A closer look at land interactions reveals that there are several ways in which land masses weaken hurricanes. The primary reason for weakening over land is that the hurricane is quickly cut off from its fuel source: the warm ocean waters. Without the warm water, the air flowing into the hurricane in Leg 1 of the Carnot Cycle (Figure 2) begins to adiabatically cool as it expands due to the lower pressure close to the eye. This process works against the heat engine by weakening the positive buoyancy needed to drive convection. By utilizing the GOES 10.7 μm satellite temperature, it is clear that landfall is quickly followed by warming cloud tops (about 2-5 $^{\circ}\text{C}$) within one to two hours of landfall as the engine shuts down (Pielke and Pielke, 1997).

The second weakening mechanism is frictional dissipation, which increases over land due to the added resistance of trees and buildings compared to the relatively smooth ocean surface. Friction acts against a typical heat engine through moving parts like pistons and gears by transferring kinetic energy into heat, which is lost to the ambient environment. In a hurricane, the only "moving part" is the winds and the only

major source of friction is in the inflow layer between the surface and the boundary layer. Over the ocean, any heat loss through frictional dissipation is simply picked up by the inflow recycled back into the system in Leg 1 of the cycle (Emanuel, 2005). Despite this energy recycling, the maximum wind speeds over the ocean are still located above the boundary layer. Over land, the friction intensifies and the surface winds are significantly impeded compared to the ocean, which once again quickly weakens the inflow in Leg 1 of the cycle.

While land interaction contributed somewhat to Gustav's weakening over Cuba, it is most pertinent to the final dissipation over Louisiana. Mountains are another factor in the Cuban landfall, as Gustav passed over peaks in the 400-600 meter range. These peaks are not as high as other islands such as Hispaniola, but they still could have impacted Gustav. Mountains are more effective than flat land at disrupting hurricanes for several reasons. First, precipitation is orographically enhanced by increased upsloping, which reduces the precipitable content within the convection. This reduces latent heat release and thus the total kinetic energy of the system. The weakening can actually be enhanced further on the lee side of the mountains as downsloping results in adiabatic compression, similar to Leg 4 of the Carnot Cycle. Finally, the localized winds flowing up, down, and around the mountains instead of purely cyclonically around the vortex can result in the entire storm becoming less organized (Bender et al., 1984).

Since the Cuban mountains were relatively low and the passage occurred quickly, it is unlikely that the mountains had a major effect on Gustav's inability to re-strengthen over the loop current. Infrared satellite images confirm that the circulation remained intact when Gustav emerged over

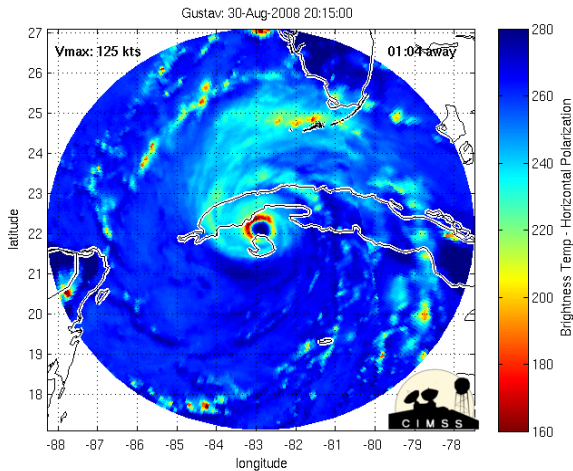


Figure 5: MIMIC Image of Gustav approaching Cuba, August 30 2015 UTC. Reproduced from UW-Madison CIMSS.

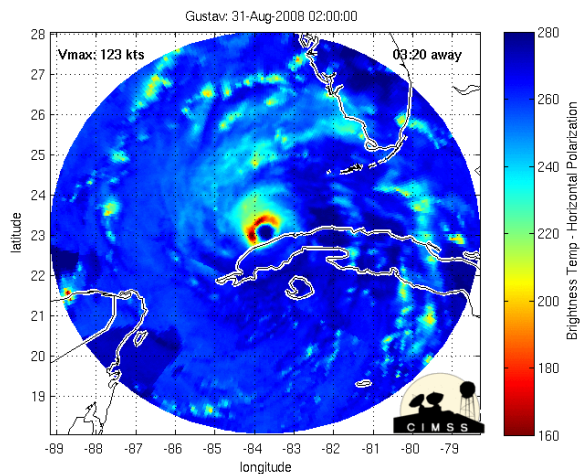


Figure 6: MIMIC Image of after emerging over the Gulf, August 31 02:00 UTC. Reproduced from UW-Madison CIMSS.

the Gulf at about 0100 UTC on August 31. Six hours later, the storm appeared to lose its axisymmetry, long after the mountains would have been a factor. MIMIC images of Gustav before and after the Cuban landfall also confirm that the circulation was relatively unaffected. Figures 5 and 6 show two MIMIC images of Gustav, one taken prior to landfall at 2015 UTC on August 30 (Figure 5) and the other taken right after emergence into the Gulf at 0200 UTC on August 31 (Figure 6). In both images, Gustav maintains a closed, circular eyewall with axisymmetric spiral bands. The bands

appear slightly weaker in Figure 6, but there was no evidence of any orographically induced weakening. These images were confirmed by observations, as in the approximately 6 hour timeframe that Gustav was over land, the maximum sustained wind only dropped 10 mph from 150 mph to 140 mph and the MSLP only rose by 6 mb.

The lack of weakening was likely due to the fact that Gustav was only over land for only 6 hours, although hurricanes have been observed to lose half of their wind speeds in seven hours after landfall on average (Emanuel, 2005). The difference with Gustav is that Cuba is a relatively narrow island and there was sufficient warm water available for inflow from the north side of the system. In landfalls over continents, the inflow from the left side of the storm (relative to propagation direction) would be drier due to continental air and slower due to friction than the inflow from the Gulf of Mexico during Gustav's Cuban landfall. The warm ocean waters on both sides of the system allowed the isothermal expansion phase to continue relatively unabated which neglected much of the negative effect of the mountains. This analysis suggests that atmospheric conditions must next be considered as the source of the unexpected weakening over the loop current.

V. Synoptic Overview

a) Upper level flow during Caribbean Intensification

Although hurricanes are self-sustaining systems that derive their energy from the ocean temperatures, the synoptic flow conditions still serve as the primary regulator that prevents storms from reaching their MPI. It is well known that vertical wind shear weakens hurricanes, but there are also general upper level patterns that are more favorable than others, even if the shear

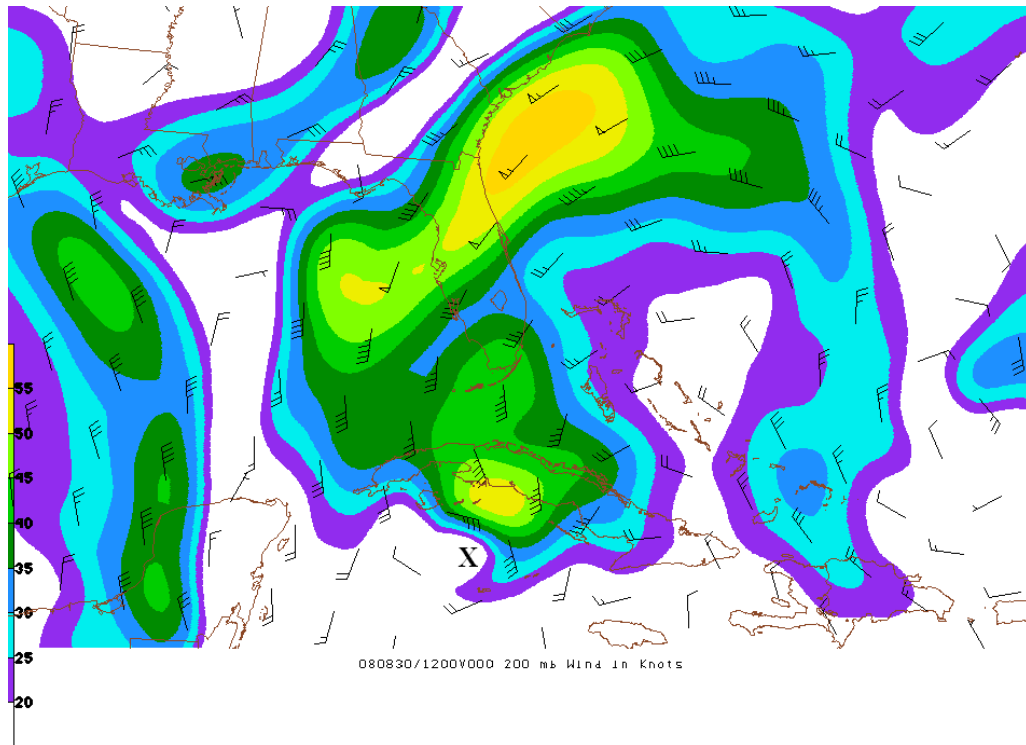


Figure 7: NAM 200 mb wind (fills) and barbs in knots, August 30 1200 UTC. A 200 mb trough is visible over the Gulf while an additional jet maximum over Cuba caused by Gustav. An “X” marks the approximate center of Gustav at the time.

is light in both scenarios. Essentially, any upper level synoptic flow regime that helps a hurricane expel its convection will encourage the storm to strengthen closer to its MPI. As established with Figure 3, the MPI is often well above the actual intensity, so a change in upper level flow can result in rapid intensification even if the ocean temperatures do not change. While a large hurricane can generally create its own outflow regime, a small, developing hurricane does not have a strong enough heat engine to push outward on the synoptic flow and expel its convection to an ideal radius. In other words, the storm can be classified as a “subcritical” vortex, meaning that outward propagating inertial gravity waves will be reflected back due to the dominating external flow (Emanuel, 1991). This is similar to the effect of an inversion reflecting downslope mountain waves, although in the case of a hurricane these waves can restrict the hurricane’s

convection as the Carnot Cycle can not operate as efficiently without ideal outflow (Tripoli, 2009).

The best upper level flow for hurricane intensification is a ridge of high pressure that coincides with the hurricane’s anticyclonic outflow. This commonly occurs under an upper level ridge with a trough approaching from the west. This process creates some weak upper level wind shear, which is actually required in a hurricane in order for advective processes such as differential vorticity advection to create synoptic scale ascent and help enhance the deep convection (Bosart et. al., 1999). The upper level ridge is consistent with negative vorticity over the hurricane from the anticyclone flow over the ridge, which expels the hurricane’s outflow due to the strong upper level divergence to the east of the trough axis. In essence, the synoptic pattern is doing mechanical work expelling the outflow, which allows the heat engine to

concentrate additional work increasing Carnot cycle. The NAM analysis of the August 30 1200 UTC 200 mb jet (Figure 7) reveals that a narrow, weak 200 mb trough was present over the Gulf of Mexico while a broad ridge extended from the Eastern Gulf to the Atlantic with a jet maximum over the Florida Peninsula. This was not an especially strong jet and it was even weaker at 300 mb, but it still places Gustav (storm center location marked with an “X”) in a favorable region for synoptic scale anticyclonic outflow enhancement. The outflow regime generated by the hurricane itself is visible over Cuba and South Florida.

This area was also associated with a large area of upper level divergence as the hurricane expelled its moisture, which coincides with the anticyclonic vorticity over the region. A secondary upper level divergence maximum associated with the jet extended from the Yucatán peninsula around the hurricane through central Florida and to the north of the Bahamas (not pictured). This divergence area likely provided the additional outflow enhancement which was essential to Gustav’s fast intensification. Water vapor images at this time reveal that this area of divergence was definitely coupled with Gustav at this point, as the storm had a broad, axisymmetric outflow that included the synoptic divergence region. The National Hurricane Center’s forecast discussion noted the potential for a trough-storm interaction on August 30 at 0600 (NHC, 2008). Gustav indeed complied with the forecast, as the maximum sustained winds grew from 110 mph at the time of Figure 7 (1200 UTC August 30) to 150 mph by August 31 at 00 UTC. From this analysis, it is clear that while the warm Caribbean Sea temperatures provided the potential for rapid intensification, it was the favorable upper level wind flow that permitted this intensification to occur.

b) Upper Level Flow during Gulf Weakening

An important caveat of the storm-trough interaction is that the synoptic conditions only remain favorable for a brief timeframe before the trough progresses eastward and vertical wind shear increases. In order to analyze these changes, it is important to note that vertical wind shear is defined as the vector difference between the upper and lower level wind flows. Traditionally, the difference between 1.5 km and 10 km is used, but it is not known exactly what shear components are most influential (Emanuel, 2005). Vertical wind shear disrupts weakens these storms by disrupting the characteristic axisymmetry of an intense hurricane. Essentially, the entire updraft in the eyewall becomes vertically tilted due to stronger winds at the upper levels. The vertically tilted updraft displace some of the convection downshear of the eyewall, which means that some of the latent heat release is also displaced downshear. According to the hypsometric equation, heating in a column will result in expansion and increased thickness, which translates to a lower column pressure. This mechanism usually acts to lower the pressure in the eyewall, but if some of the convection is displaced downshear, the pressure reduction will be spread over a larger area and the hurricane will lose some of its intensity (Emanuel, 2005 and Tripoli, 2009). In some cases, the convection can be completely removed from the upshear side of the hurricane, which literally means the hurricane was ripped apart.

A computer simulated cross section of shear during a hurricane is shown in Figure 8. The arrows represent the radial wind and the shading is the strength of the wind blowing around the eye. Figure 8a (left side) reveals that a storm with weak wind shear is relatively axisymmetric with vertically oriented convection. In figure 8b

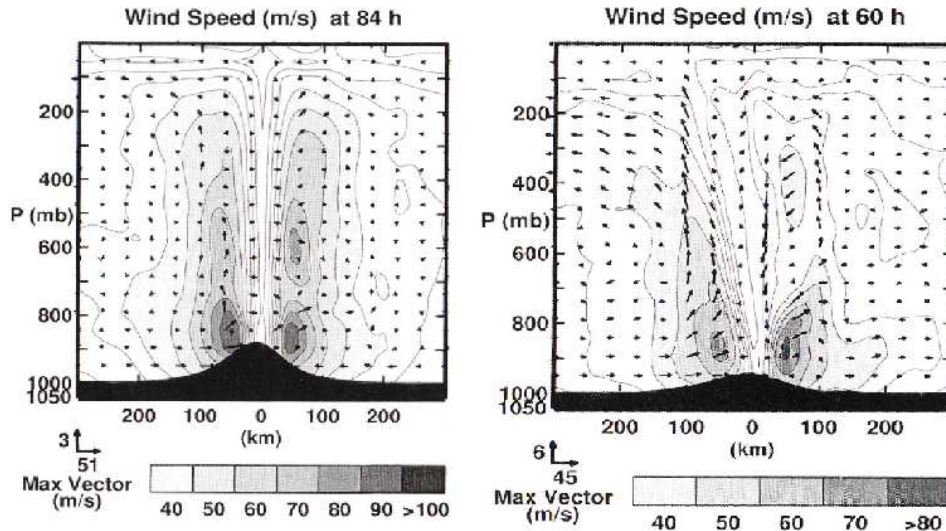


Figure 8a (left) and 8b (right): Computer simulated cross section of vertical and radial wind (arrows) and rotation around the storm's axis (fills). The x-axis shows the radial distance from the center of circulation. An example with weak wind shear (left) shows a symmetric circulation while strong wind shear from right to left (right) shows the rotational winds skewed toward the downshear side of the storm

(right side), shear orientated from right to left results in weaker convection on both sides, with the stronger convection on the downshear side of the storm and weak convection on the upshear side. In addition, the eyewall experiences a downshear tilt. This confirms that a storm experiencing shear should lose its symmetry and have the strongest convection displaced downshear (Emanuel, 2005).

Although Gustav never experienced dramatic shear, it is important to make some shear calculations to determine if an increase in shear contributed to Gustav's weakening over the Gulf of Mexico. For the shear analysis, NAM 104 analysis maps from 850 mb and 300 mb were used since they are closest to 1.5 km and 10 km elevation. For reference, the shear over the Caribbean at August 30 1200 UTC was first examined. Shear was less than 10 knots on all sides of the storm at this time, which coincides with previous analysis that conditions were favorable for strengthening. When the storm was over the loop current 24 hours later on August 31 1200 UTC, the shear remained

negligible except on the south and especially west sides of the storm. The shear was almost exclusively between 500 and 300 and appeared to be related to the upper level trough that was still present over the western Gulf. The winds around west side of the hurricane naturally flow cyclonically from a northerly direction, but the eastern edge of the trough shifted winds to a southerly direction at upper levels. This resulted in shear vectors coming from the south to southwest at 15-20 knots. A GOES 12 6.7 μm water vapor imagery from this time (Figure 9) shows the upper level trough clearly present over the western Gulf as an area of dry, continental air. Gustav's outflow is extensive on the east side of the storm, reaching out into the Atlantic while the western outflow is being restricted by the existence of this trough.

The water vapor image does not suggest, however, that the shear is displacing convection from the lower level circulation. Gustav was much more disorganized at this point than it was when it emerged off of Cuba, as the eye is no longer

visible on satellite imagery and the deep convection is not asymmetric. The shear is unlikely the direct source of this disorganization, as the deep convection is more prominent on the south side of the circulation while convection on the north side of the eye is warmer and frayed. This is not expected from a south to southwesterly sheared storm, as the deeper convection should be to the north or northeast according to the model runs in Figure 9. Therefore, it is likely that shear had a more subtle effect on the circulation and was not primary cause of the weakening over the loop current.

c) Continental Air Mass Entrainment

As noted in the shear discussion, a dry continental air mass coincided with the upper level trough over the western Gulf. Dry air masses are often detrimental to hurricane intensity, as shear can force dry, low θ_e air into the circulation at middle levels. This has a similar effect as the other weakening mechanisms, as the dry, continental air has less entropy than the high θ_e air that originates from the low level moist inflow. This acts to disrupt Leg 2 of the Carnot cycle by mixing out some of the moist air ascending in the eyewall at mid levels. The mixing warms the effective cold reservoir temperature (T_f in Figure 2) closer to the mid level ambient temperature, which can significantly reduce the efficiency of the heat engine and weaken the total energy of the storm. This process is further accelerated if the high convective cloud tops are dissipated, as more infrared radiation is allowed to escape to space. This acts as a feedback mechanism which further removes heat from the core of the storm and weakens the Carnot cycle (Emanuel, 2005). Importantly, only weak wind shear is needed for dry air entrainment if the dry air source is located in close proximity to the hurricane.

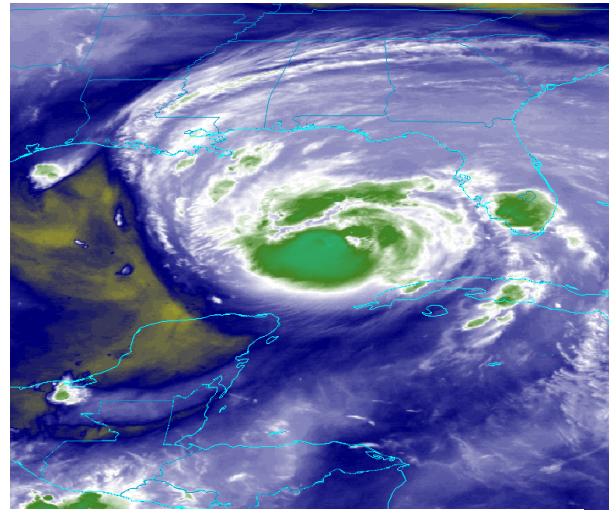


Figure 9: GOES 12 6.7 μm water vapor image, August 31, 1200 UTC. Dry upper level air is visible as yellow and dark blue while moist upper level air is green and white.

From the water vapor image in Figure 9, it is apparent that dry air is being wrapped into Gustav's vortex. The driest air is still located in the western Gulf, but a ribbon of relatively low moisture is seen wrapping around the south side of the vortex and into the eastern side of the storm. Figure 10 shows the August 31 12 UTC 500 mb θ_e AVN211 model analysis. From this plot, it is clear that the low θ_e air from the trough is wrapping completely around Gustav's vortex and into the eyewall. This "tongue" of dry air has resulted in a highly asymmetric mid level θ_e profile, as the 346 K θ_e contour extends outward to the north of the center of circulation while the 344 K contour wraps around below it to the north of the eyewall. This analysis strongly correlates with Figure 9, as the lack of deep convection to the north of the center of circulation is associated with low 500 mb θ_e values and the deep convection to the south of the eyewall is associated with higher θ_e values. Even after Gustav crossed Cuba, it still had a much more symmetric 500 mb θ_e profile (not pictured) than the one seen in Figure 10.

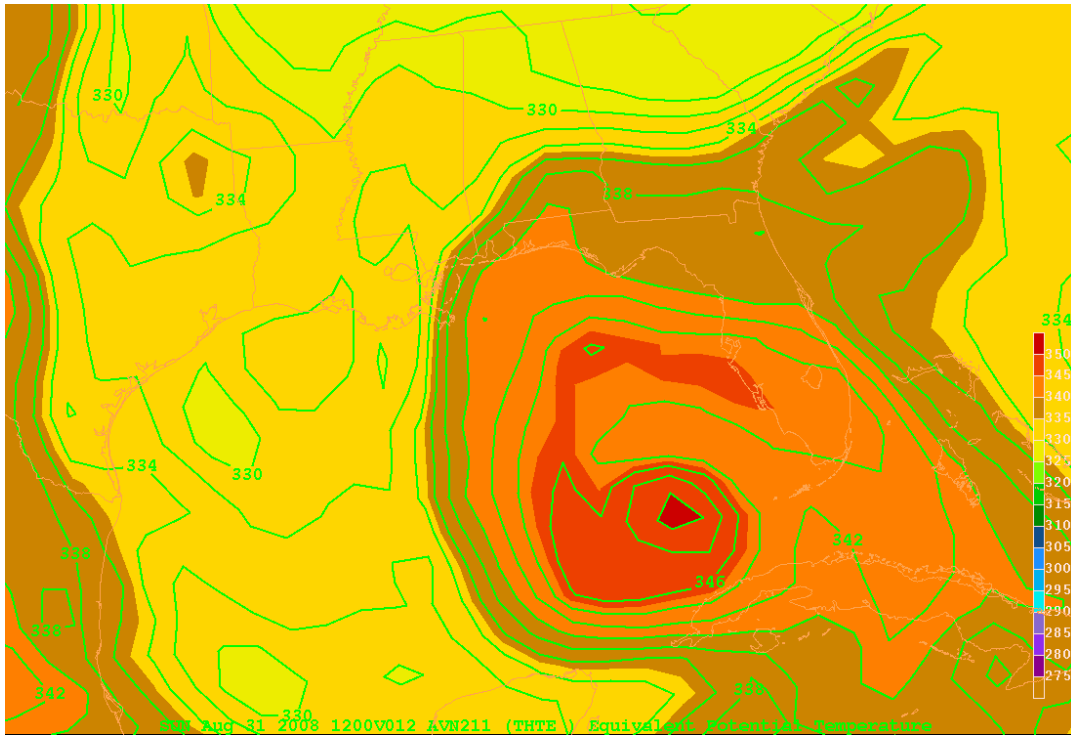


Figure 10: AVN 211 model 500 mb Equivalent Potential Temperature (θ_e), August 31 1200 UTC. The “tongue” of dry air is causing the asymmetric θ_e profile in Gustav.

This dry air entrainment is definitely the primary mechanism that weakened Gustav from 130 knot maximum sustained winds at 00 UTC August 31 to 110 knot maximum sustained winds just 12 hours later at 1200 UTC August 31, despite the storm passing directly over the loop current during this time period. Gustav did eventually manage to partially fight off the dry air entrainment and regain some of its asymmetry, but this did not occur until late August 31 and early September 1, by which time Gustav had moved into ocean waters with a much lower TCHP (Figure 4). Remarkably, the decrease in intensity caused by dry air entrainment was even more significant than the 10 knot maximum sustained wind drop that occurred from the passage over the landmass of Cuba, which suggests that in at least this case, atmospheric conditions have a greater influence on hurricane intensity than a six hour pass over a landmass.

VI. Mesoscale Analysis:

a) Eyewall Replacement Cycle in north Gulf of Mexico

A full dynamical explanation of eyewall replacement cycles remains elusive, but they frequently occur in mature tropical cyclones and result in perceptible intensity fluctuations. Eyewall replacement cycles arise when a tropical cyclone’s spiral bands organize into a secondary eyewall with a radius larger than the original eyewall. As this new vorticity maximum organizes, it cuts off the inflow from the inner eyewall, causing the inner eyewall to spin down and resulting in the new eyewall taking over (Camp and Montgomery, 2000). One possible explanation for the formation of these outer vorticity maxima involves the creation of Rossby waves within the hurricane vortex. These waves can transport momentum outward from the center of the storm which potentially can organize into

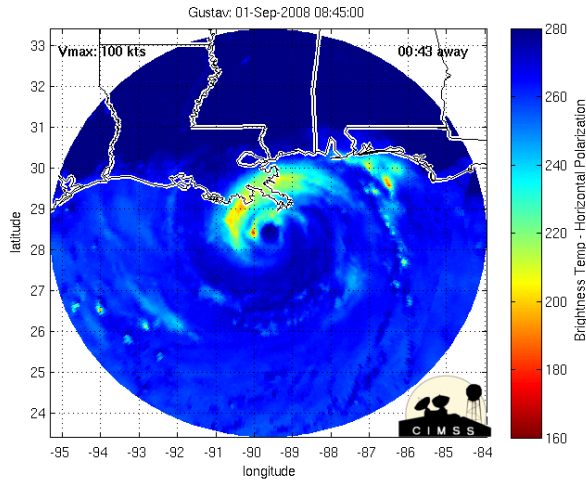


Figure 11: MIMIC Image of Gustav with concentric eyewalls, September 1 0845 UTC. Reproduced from UW-Madison CIMSS.

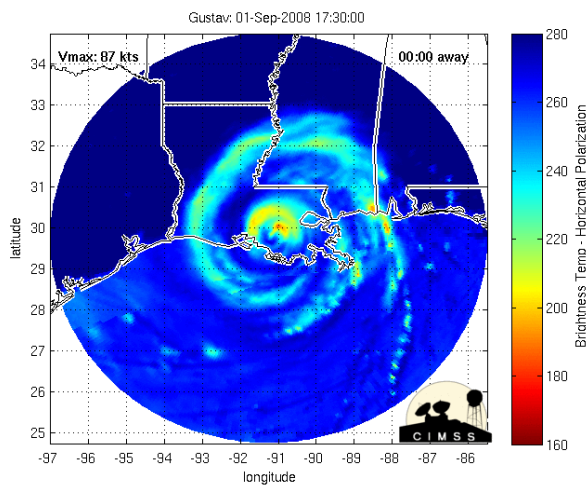


Figure 12: MIMIC Image of Gustav with the outer eyewall gradually eroding the inner eyewall, September 1 1730 UTC. Reproduced from UW-Madison CIMSS.

this secondary vorticity maximum (Tripoli, 2009). The Rossby waves form through moist convective processes and are larger than inertia-gravity waves, as they have a Rossby radius of deformation on the same scale as the tropical cyclone itself.

While eyewall replacement cycles have been created without any external forcing, a second method of formation is proposed involving interaction with synoptic features. It is proposed that an external cyclone vorticity perturbation associated with a synoptic scale upper level trough,

which is also a Rossby wave, could interact with the spiral bands. This interaction would create a new vorticity anomaly in one of the bands, which would then grow to overtake the previous inner eyewall (Nong and Emanuel, 2003). It is not known exactly which formation mechanism is correct, but the impacts on intensity are well known. These cycles are another aspect of hurricanes that keeps these storms from reaching their MPI and results in intensity fluctuations that are difficult to forecast. As the outer eyewall first takes over the inner eyewall, the intensity has been observed to decrease, but as the new eyewall contracts and takes over, the hurricane can once again experience significant intensification (Willoughby et. al., 1982).

Locating eyewall replacement cycles without radar data is difficult, but the MIMIC images provided a very effective substitute. Gustav may have underwent an eyewall replacement cycle just before it reached its peak intensity in the Caribbean, but it is difficult to tell with the available analysis. In the north Gulf of Mexico, Gustav underwent at least one eyewall replacement cycle according to the MIMIC analysis. These cycles were relatively minor, as the first possible cycle that appeared to occur late on August 31 did not affect the maximum sustained wind according to the NHC. This cycle will not be analyzed as part of this discussion, since the eyewall may have simply appeared concentric due to the spiral of low θ_e air that was wrapping into the system. The fact that there was no change in the intensity further suggests that this was not an eyewall replacement cycle.

The second eyewall replacement cycle began around 0400 UTC on September 1 and was still in progress when the storm made landfall around 1400 UTC September 1. At the beginning of the cycle, Gustav had managed to fight off some of the θ_e entrainment and had regained a nearly

symmetric central dense overcast. Only the MIMIC was considered for this analysis since the eye never reemerged in satellite imagery and the New Orleans radar imagery was too far away to capture the beginning of the replacement cycle. Figure 11 shows the storm near the beginning of the eyewall replacement cycle at 0845 UTC on September 1. Gustav was still asymmetric at this point but had reorganized into concentric eyewalls that are well defined on the north side of the storm. Figure 12 shows Gustav later that night at 1730 UTC. Two eyewalls were still present at this point, but the outer eyewall had contracted and appeared to be taking over the weaker inner eyewall. This shows that the cycle was not yet complete as landfall occurred, so re-intensification never happened.

Gustav began the replacement cycle with maximum sustained winds of 115 mph, made landfall with 110 mph winds, and had winds reduced to 90 mph by the time of Figure 12. It is possible that this reduction was due to the eyewall replacement cycle, but dry air entrainment was once again apparent in the water vapor imagery prior to landfall so it is difficult to pinpoint which effect actually caused the weakening. Of course, the TCHP was also lower right along the coast, which could have also factored into the weakening. Still, this case does show that importance of further understanding eyewall replacement cycles. The cycles usually take about a day to complete, but had the cycle occurred slightly faster, Gustav may have experienced strengthening before landfall and been stronger instead of weaker than the official forecasts.

VII. Conclusion:

As with any major hurricane, Gustav experienced a number of environmental and dynamical interactions that resulted in many

intensity fluctuations. The conceptual model of a Carnot heat engine works well to understand the environmental interactions, but internal dynamic fluctuations such as eyewall replacement cycles continue to pose conceptual challenges. As a result, the National Hurricane Center forecast track was accurate several days in advance while the intensity forecast underestimated the Caribbean strengthening and overestimated intensity over the loop current as well as the final intensity. The storm was always forecasted to be a major hurricane at the Louisiana landfall when it in fact made landfall as a Category 2 storm (NHC, 2008).

After analysis, it was determined that the synoptic environment was the primary aspect that determined Gustav's intensity. The Tropical Cyclone Heat Potential of the ocean provided a basis for the maximum potential intensity (MPI), but the actual intensity was well below the MPI. The ocean heat content was very high as Gustav passed over both the northern Caribbean and the Gulf of Mexico loop current, but the storm intensified over the Caribbean due to a favorable storm-trough interaction that enhanced outflow while it weakened over the loop current due to increased southwesterly shear and dry air entrainment. The internal dynamics associated with eyewall replacement cycles also may have prevented Gustav from strengthening prior to landfall, although the results were inconclusive.

With increased buildup along ocean coastlines, the stakes have never been higher for intensity forecasts. Gustav's strong winds, storm surge, and heavy rains caused an estimated \$4.3 billion dollars worth of damage in Louisiana even though it weakened prior to landfall (NHC, 2008). The evacuation also had an additional impact, as 1.9 billion people evacuated southern Louisiana due to concern that a Katrina repeat was imminent (NOLA,

2008). Since Gustav was not as strong as anticipated, some of these evacuations could have been avoided with better forecasts. It is believed that incorporation of microwave imagery into hurricane forecasting could help improve these forecasts as well as assist meteorologists in developing a better dynamical understanding of hurricane intensity fluctuations.

VIII. Acknowledgements:

This project would not have been accomplished without my UW-Madison AOS 453 classmates who helped with this case study by answering various questions and helping with technical difficulties in generating images. Pete Pokrandt was especially helpful for retrieving model data and radar data for use in this study. Dan Henz provided much assistance by answering various questions about hurricanes and helping direct me to the eyewall replacement cycle over Cuba. Finally, UW-Madison Professor Greg Tripoli (cited in paper as Tripoli, 2009) helped me understand vertical wind shear, storm-trough interactions, and eyewall replacement cycles.

IX: References:

Anderson, E., 2008. *1.9 Million People Evacuate South Louisiana*. NOLA.com Hurricane News and Storm Trackign. <http://www.nola.com/hurricane/index.ssf/2008/08/11_million_people_evacuate_sou.html> Accessed 4 May 2009.

Atlantic Oceanographic and Meteorological Laboratory, 2008. *Tropical Cyclone Heat Potential Home*. <<http://www.aoml.noaa.gov/cgi-bin/trinanes/searchmaps1.cgi?month=8&day=28&year=2008>> Accessed May 4, 2009.

Bender, M.A., R.E. Tuleya, Y. Kurihara, 1984. A Numerical Study of the Effect of a Mountain Range on a Landfalling Tropical Cyclone. *Monthly Weather Review*, **113**, 567-583.

Bosart, L.F., C.S. Velden, W.E. Bracken, J. Molinari, P.G. Black, 1999. Environmental Influences on the Rapid Intensification of Hurricane Opal (1995) over the Gulf of Mexico. *Monthly Weather Review*. **128**, 322-250.

Camp, J.P. and M.T. Montgomery, 2000. Hurricane Maximum Intensity: Past and Present. *Monthly Weather Review*. **129**, 1704-1717.

Cooperative Institute for Meteorological Satellite Studies, 2008. *Hurricane Gustav*. CIMSS Tropical Cyclones Image Gallery.<<http://cimss.ssec.wisc.edu/tropic/archive/2008/storms/gustav/gustav.html>> Accessed 4 May 2009.

Emanuel, K., 1991. Current understanding of tropical cyclone structure and intensity changes – a review. *Annual Rev. Fluid Mech.* **87**, 257-278.

Emanuel, K., 2005. *Divine Wind: The History and Science of Hurricanes*. Oxford University Press, 54-80.

Holton, J.R., 1979. *An Introduction to Dynamic Meteorology*. 3rd. Ed. Academic Press.

National Hurricane Center, 2007. *Glossary of NHC Terms*. <<http://www.nhc.noaa.gov/aboutgloss.shtml>> Accessed 4 May, 2009.

National Hurricane Center, 2008. *Gustav Graphics and Advisory Archive*.

<http://www.nhc.noaa.gov/archive/2008/graphics/al07/loop_5W.shtml> Accessed 4 May, 2009.

Nong, S.Y. and K.A. Emanuel, 2003. A numerical study of the genesis of concentric eyewalls in hurricanes. *Q. J. R. Meteorol. Soc.* **129**, 3323–3338.

Pielke, R.A Jr. and R.A. Pielke, Sr., 1997. *Hurricanes: their Nature and Impacts on Society*. John Wiley and Sons: West Sussex.

Shay, L.K., G.J. Goni, P.G. Black, 1999. Effects of a Warm Oceanic Feature on Hurricane Opal. *Monthly Weather Review* **128**, 1366-1383.

Wang¹, Y. and C.C. Wu, 2004. Current understanding of tropical cyclone structure and intensity changes – a review. *Meteorol Atmos Phys.* **87**, 257–278.

Willoughby, H.E., J.A. Clos, and M.G. Shoreibah (1982): "Concentric eye walls, secondary wind maxima, and the evolution of the hurricane vortex" *J. Atmos. Sci.*, 39, pp.395-411.